Review of Scientific Instruments

An experimental setup for dip-coating of thin films for organic solar cells under microgravity conditions

Cite as: Rev. Sci. Instrum. **92**, 015108 (2021); https://doi.org/10.1063/5.0018223
Submitted: 12 June 2020 . Accepted: 10 December 2020 . Published Online: 05 January 2021

Leif K. E. Ericsson, Ishita Jalan, Alf Vaerneus, Thomas Tomtlund, Maria Ångerman, and Jan van Stam

Review of Scientific Instruments ARTICLE scitation.org/journal/rsi

An experimental setup for dip-coating of thin films for organic solar cells under microgravity conditions

Cite as: Rev. Sci. Instrum. 92, 015108 (2021); doi: 10.1063/5.0018223
Submitted: 12 June 2020 • Accepted: 10 December 2020 •
Published Online: 5 January 2021

Leif K. E. Ericsson,[1,a] Ishita Jalan,[2,b] Alf Vaerneus,[3,c] Thomas Tomtlund,[3,c] Maria Ångerman,[3,c] and Jan van Stam[2,b]

AFFILIATIONS

[1] Department of Engineering and Physics, Karlstad University, Universitetsgatan 2, SE-651 88 Karlstad, Sweden
[2] Department of Engineering and Chemical Sciences, Karlstad University, Universitetsgatan 2, SE-651 88 Karlstad, Sweden
[3] Swedish Space Corporation, P.O. Box 4207, SE-171 04 Solna, Sweden

[a] **Author to whom correspondence should be addressed:** leif.ericsson@kau.se
[b] **Electronic addresses:** ishita.jalan@kau.se and jan.van.stam@kau.se
[c] **Electronic addresses:** alf.vaerneus@sscspace.com; thomas.tomtlund@sscspace.com; and maria.angerman@sscspace.com

ABSTRACT

We report the design and testing of a custom-built experimental setup for dip-coating from volatile solutions under microgravity conditions onboard an aircraft. Function and safety considerations for the equipment are described. The equipment proved to work well, both concerning the safety and the preparation of thin films. No leakage of the solvents, nor the solvent vapors, was detected, not even in a situation with a fluctuating gravitational field due to bad weather conditions. We have shown that the equipment can be used to prepare thin films of polymer blends, relevant for organic solar cells, from solution in a feasible procedure under microgravity conditions. The prepared films are similar to the corresponding films prepared under 1 g conditions, but with differences that can be related to the absence of a gravitational field during drying of the applied liquid coating. We report on some introductory results from the characterization of the thin films that show differences in film morphology and structure sizes.

I. SCIENTIFIC INTRODUCTION

Organic solar cells (OSCs) is an interesting alternative to other techniques to produce renewable energy. This field has gained much attention as it promises low-cost, flexible, and aesthetically pleasing solar energy harvesting devices.[1–6] Solution processability of materials allows, for example, the possibility to use roll-to-roll printing adapted from the printing industry for the large-scale production of organic solar cells.[7]

OSCs are multilayered semiconducting devices,[8,9] consisting of a photoactive layer between two electrodes. There are often an electron transport layer and a hole transport layer between the active layer and the two electrodes, respectively. The active layer is prepared using a one-step process from a ternary solution of two non-volatile solutes (the electron donor and the electron acceptor) and one volatile solvent, leading to the bulk heterojunction (BHJ) morphology.[8,9] It is important to understand how the evaporation of the solvent impacts the distribution of the two non-volatile components and, hence, the morphology of the dry, thin solid film, i.e., the active layer. The morphology has a profound impact on the exciton diffusion and charge transport properties[10–12] of the device and, consequently, on the device efficiency.

To control the morphology, one needs to understand the morphology formation process on a molecular level. It is known that the final morphology can be altered by the choice of solvent, the blend ratio of the donor and acceptor, the total concentration of dissolved species, or by the use of additives.[10,11,13–16] The Flory–Huggins interaction parameters govern morphology formation and

purity of domains of blended polymers and small molecules.[13,17,18] These interaction parameters between the solute–solute and solute–solvent are key to understanding how the donor–acceptor blend phase separates.

As the solvent evaporates, a concentration gradient develops. Due to this gradient and the short drying time, a partial phase separation will occur during the formation of the thin film. The solvent evaporation process is fast, and the final morphology is a frozen, non-equilibrium state. It is a challenge to study the early stages of the phase separation at 1 g conditions due to the complexity of the interactions and dynamics involved in the drying process of a polymer blend solution. At 1 g, the convective effects dominate and partly hide the phase separation processes, whereas in microgravity, Marangoni flow and capillary flow will be the dominant sources of mass transport during solvent drying.[19] Phase separation is also known to slow down under microgravity conditions,[20,21] and there is experimental evidence for differences in structure between thin films prepared at 1 g and those prepared under microgravity conditions.[22,23] The slower kinetics will extend the timescale for phase separation, and the process can be studied in more detail, especially in its early stages. Therefore, performing the coating and drying under microgravity conditions gives us the opportunity to study the process at different timescales. One of the main problems to achieve this is the practical difficulties connected to performing wet-chemistry depositions in a safe and reliable way under microgravity conditions during a parabolic flight campaign.

This contribution reports on the design and testing of a custom-built experimental setup for dip-coating under microgravity conditions onboard an aircraft. Function and safety considerations for the equipment are described. We have shown that the equipment can be used to prepare thin films of polymer blends from solution in a safe and reliable way under microgravity conditions. We used a well-studied model system[1,14,24–26] of poly[2,3-bis-(3-octyloxyphenyl)quinoxaline-5,8-diyl-alt-thiophene-2,5-diyl] (TQ1)[27] and [6,6]-phenyl-C_{70}-butyric acid methyl ester ($PC_{70}BM$) made from solutions in different solvents.

The results presented here show that the custom-designed equipment works as intended and that the dip-coated films can be produced under microgravity conditions. This also shows the possibility to transfer OSC production from Earth conditions to space conditions, a research field that presently is at an early stage with, to our knowledge, only two reports on exploring the use of OSCs in space applications.[28,29] We also report on some introductory results from the characterization of the thin films that show differences in film morphology and structure sizes. These differences can be related to the gravitational field effects.

A. Safety and risk introduction

A custom-designed equipment was built to facilitate studies of the impact from microgravity as compared to Earth conditions. The equipment enabled experiments involving flammable and volatile solvents onboard an airplane. This involves challenges regarding the combination/competition between function, ease of use, and safety, of which the latter is the one that can never be negotiated.

The equipment was tested in flights, and the first scientific study was done during the 70th ESA Parabolic Flight Campaign, VP 140, in Merignac, France, on October 2018 with a Novespace Airbus A310 ZeroG aircraft. The campaign was performed over three days, with each day containing 30 experimental parabolas. The 30 parabolas are divided into six sets of five parabolas each, with a short break between each set. Each parabola sequence starts with a pull-up phase with hypergravity at 1.5 g–1.8 g for about 24 s, during which the airplane goes from steady horizontal flight to 47° climb. At this position, called injection, the engine thrust is reduced, and the airplane makes an ~22 s long parabola with microgravity (~5×10^{-2} g), ending with a 47° descent where the engines are engaged again. The last part of the sequence is a pull-out phase with hypergravity at 1.5 g–1.8 g where the airplane ends in steady horizontal flight at 1 g.

The primary challenge in the design process for the equipment was to enable reliable and reproducible dipping of substrates in volatile solutions without releasing solvent vapors in the airplane cabin. This calls for a mechanism that opens and closes solution vials and, since the vials are open for a short time, a second containment to prevent vapors from leaking to the cabin. Due to the requirements for a rigid design in the flight configuration, such a second containment naturally becomes opaque. Consequently, surveillance systems to monitor the equipment and ventilation to avoid explosive solvent vapor/air mixtures are needed for a safe configuration. In addition, a possibility to check the integrity of the solution vials before any power is turned on is needed.

II. EQUIPMENT DESCRIPTION AND PERFORMANCE

The equipment used for this experiment was designed and built as a collaboration between the Swedish Space Corporation (SSC) and Karlstad University (KaU) with valuable inputs from Novespace, France. The final assembly and testing were done at KaU. The flight equipment consists of two main parts, one control rack and one closed experimental box as shown in Fig. 1. The former holds all control electronics, while the latter is a closed, but ventilated, 259 l aluminum Zarges box (ZARGES GmbH, Germany) that contains all moving parts in the form of two dipping units (DUs) and

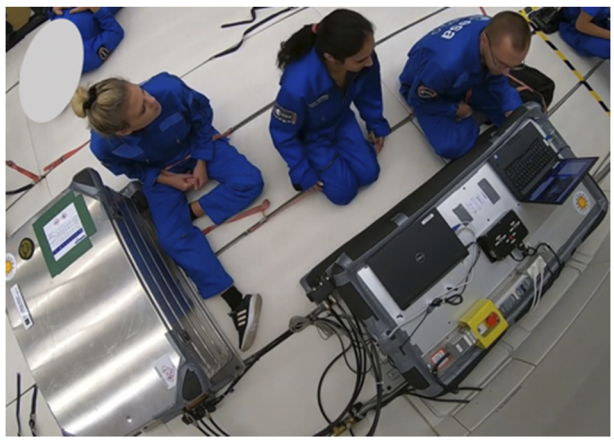

FIG. 1. Photograph from the flight configuration in the 70th ESA PFC, VP 140, showing the control rack to the right and the experimental Zarges box to the left.

surveillance cameras with illumination. The two DUs and their control equipment are completely separated so that one unit can still be used, even if any functionality of the other is lost.

The control rack carries two laptop computers and control switches, one setup for each DU, as well as all electronics for controlling the DUs. Airflow rotameters for surveillance and control of the ventilation of the Zarges box are also mounted on the control rack. The Zarges box, interior shown with a drawing and photograph in Fig. 2, contains two identical DUs and two racks for storage of substrate holders, called forks. The forks carry five glass substrates each, which are to be dipped in solutions for thin film preparation. In addition, the Zarges box contains video cameras and illumination, shown in Fig. 3, enabling monitoring of the two DUs during experiments when the Zarges box is closed. The Zarges box is ventilated through the airplane ventilation to the outside of the plane.

The experiments were performed under ambient conditions onboard the aircraft. For example, the temperature during the experiments follows the temperature in the aircraft, which is close to room temperature.

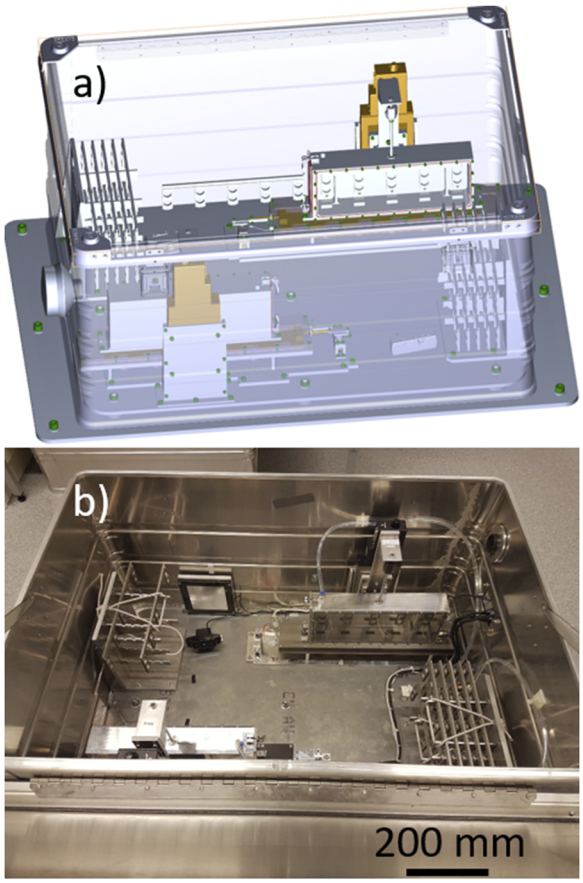

FIG. 2. (a) Drawing of the experimental Zarges box, and (b) photograph of the interior.

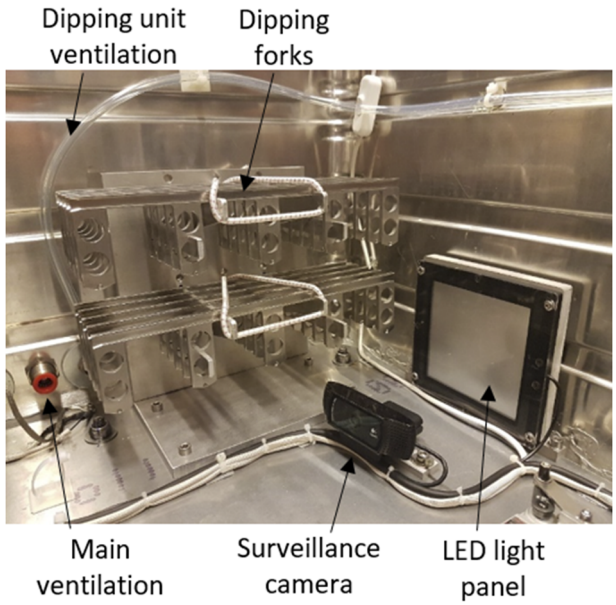

FIG. 3. Detail of the Zarges box interior showing one of the fork racks, camera, and LED light panel for surveillance of one DU. Connections for ventilation are indicated. The forks are 280 mm long (scale reference).

A. Experimental dipping units

A dipping unit, shown in Fig. 4, carries five glass vials for dipping solutions, each with a maximal volume of 12 ml. The vials are mounted on an aluminum base plate and fixed by a PEEK plate on top. The PEEK plate is mounted together with an anodized aluminum plate, making up a sealed unit for a sealing slider. A servomotor moves the slider between the open and closed positions, allowing dipping of the substrates in the solutions in the open position.

An FPM O-ring seals the vials against the PEEK plate as a primary seal. On top of the PEEK plate, the sealing slider, sliding between the PEEK plate and the anodized aluminum plate, shuts the vials by putting pressure on the FFKM O-rings when in the closed position, as shown in detail in Fig. 5. The tapered sections on the anodized aluminum plate push the slider against the FFKM O-rings to ensure a proper seal. The aluminum plate and the PEEK plate are held together by torque-tightened bolts to ensure an evenly distributed force and hence an efficient seal. A second larger FPM O-ring between the PEEK plate and the aluminum plate circumferences the primary seals in order to prevent leakage in case of failure of any of the primary FFKM O-rings. On top of the aluminum plate, the fork housing is mounted, built as an aluminum box with one wide side made of transparent polycarbonate plastics. The dipping movement and the integrity of the glass substrates are monitored through this window using one camera per DU. The glass substrates for dipping are attached to the fork with a screw and an O-ring in order to apply an even pressure on the glass and avoid cracks. The forks slide into a holder, which, in turn, is connected to a rod sticking out of the top of the aluminum housing through an O-ring sealed opening.

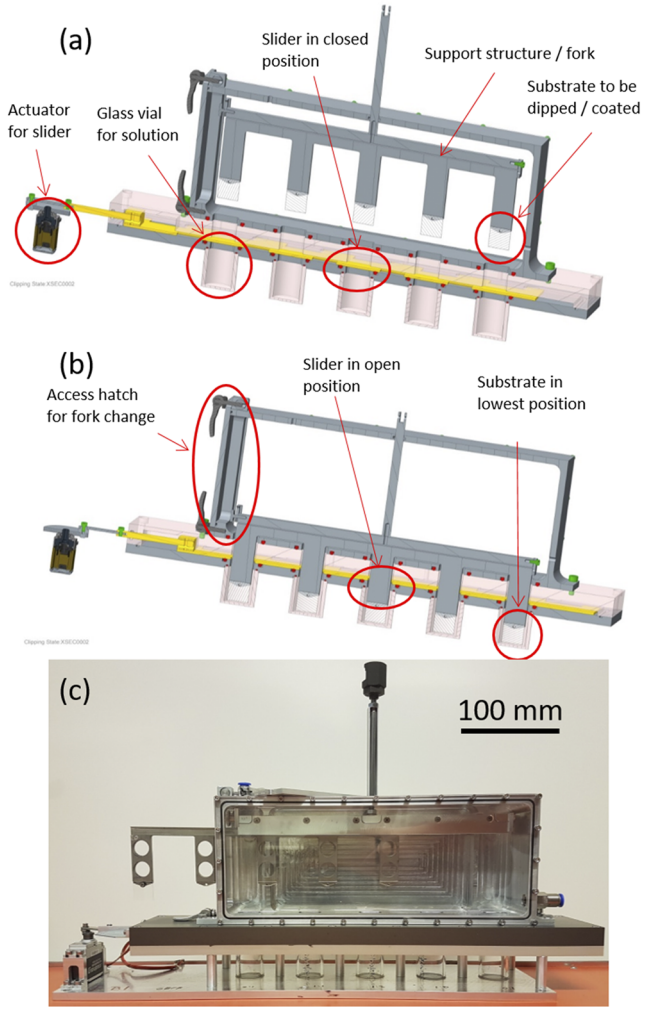

FIG. 4. (a) and (b) Drawing of a dipping unit in two different positions with essential parts indicated. Aluminum base plate is not shown. (c) Photograph of a dipping unit with the fork pulled out for fork change. One glass substrate is seen mounted on the far-left fork part. Quick connection for the ventilation is seen on the top left corner, and the check valve for air flowing in on the right-hand side.

At the end of the rod is a connector, seen in Fig. 4(c), which allows adjustment and a safe connection to the linear drive.

During the break between two parabola sets, the forks with the coated glass substrates are replaced by the fresh ones. This is done by removing the hatch at the short end of each DU after opening the quick locks [Fig. 4(b)], unlocking the fork from its holder, withdrawing the fork with the coated substrates, and placing it in the holder for the used forks inside the Zarges box. A new fork, one for each DU, with uncoated glass substrates is taken from the holder for fresh forks in the Zarges box and is mounted and locked in the holder, and the hatch is closed. Note that the Zarges box is open to the aircraft cabin during this operation.

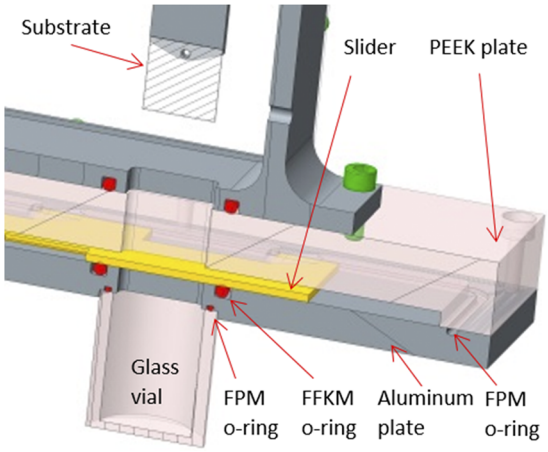

FIG. 5. Detail showing the sealing concept for the glass vials.

B. Solvent leakage safety system and ventilation

To prevent any leakage of hazardous liquids or vapors to the aircraft cabin, several safety functions were designed. The safety is based on a two-stage containment of the hazardous solvents used in the experiment. The first containment is the DU, while the Zarges box, with sealed joints, makes up the second containment. In this manner, any solvent escaping from the experiment vials into the upper part of the DUs, e.g., due to negative gravity during flight, is still kept within the first containment. In such a case, the unit with solvent in the upper part is closed for the experiment for the rest of the flight day while the other DU still can be used. The second containment, the Zarges box, prevents any solvent from leaking out in the aircraft cabin in the event that the first containment fails.

Two scenarios were foreseen as a failure of the first containment: damage to the upper part of the DU and leakage from one or more of the vials. If any of these would occur, the hazardous solvent may be released in the Zarges box with a potentially explosive air/solvent mixture as a result. Such a dangerous situation is prevented by a connection from the Zarges box to the aircraft ventilation. The aircraft ventilation is driven by the differential pressure between the cabin and the outside, with the outside pressure being typically 300 mbar at the steady-flight level between the parabolas. The maximum allowed ventilation flow, also used as the design flow, was 200 l/min.

Both the DUs and the Zarges box have ventilation connections to the aircraft ventilation, as shown schematically in Fig. 6. The ventilation is divided into three lines, one to each DU and one ventilating the Zarges box. Each line has its own rotameter to enable the verification of the flow before opening the Zarges box or performing coating experiments. The default setting is that all ventilation lines are open to continuously evacuate solvent vapors. During the drying sequence, however, airflow around the substrates could cause unwanted turbulence. Consequently, the ventilation of the upper parts of the DUs is closed when dipping is initiated and opened again after the parabola is completed. This procedure is only occasionally changed after the last set of parabolas. In order to perform the so-called vapor annealing, which is letting the substrates dry in

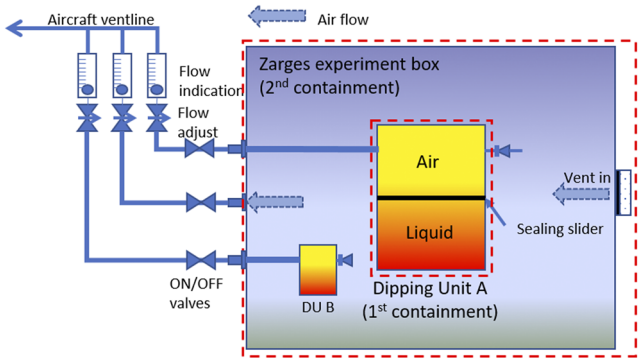

FIG. 6. Schematic drawing of the containments and the ventilation. A dipping unit that consists of the sealed vials and the upper compartment for the forks makes up the first containment. This sealed unit is leak tight even if the sealing slider is open, meaning that the sealed vials can be viewed as the zeroth containment.

a solvent vapor atmosphere, the ventilation of the DU is closed until the aircraft starts its descent back to landing. The only reason for having ON/OFF valves installed is for the occasion if a DU breaks down and releases solvents in the Zarges box during flight. In such a case, these valves can be closed while the Zarges box is removed from the aircraft and brought to a safe place on ground. The Zarges box is equipped with a filter, Sundstrom SR 297 (Sweden), to allow pressure equilibration between the box and the aircraft cabin, but preventing solvent vapors to escape to the cabin. Both the DUs have a check valve that allows air to enter the DUs from the Zarges box interior, thereby avoiding any substantial differential pressure in the DUs.

The main design parameter, in addition to the dipping function, was the safety concerning containment of solvent liquid and vapor. Four DUs were built and adjusted individually with spacer washers to ensure sealing as well as a smooth slider motion. During the assembly phase, the integrity of the vials was tested by two methods. By filling the vials with ethanol and placing the DUs upside down with the sealing slider closed, no leakage could be detected. In addition, the design was tested by placing a DU in a vacuum chamber for several hours with ethanol in the sealed vials. No loss of ethanol could be detected. The above-described tests confirmed that the slider sealed the vials efficiently when in the closed position, and the DUs were thus considered tight when the slider was in the closed position during flight. This was also confirmed in the flight since no solvent smell could be detected when the Zarges box was opened for fork exchange.

To test the sealing of the vials, the DUs were turned upside down prior to every flight with the vials filled with the experiment solutions. This test was evaluated by looking for leaks and smelling around the vials (all solvents used in the flight campaign were easily detected by smelling). At one occasion, one DU was taken out from the flight schedule due to a failed leak test. Evaluation on ground revealed that one O-ring was mounted wrong.

C. Experiment control and monitoring

All control and monitoring of the experiment is done from the control rack where the main parts are two laptop computers, one for each DU, two communication boxes for the linear drives, and one switch control box for the servomotors in the DUs.

The main safety functions during flight are camera surveillance of the two DUs and monitoring and control of the ventilation flow, as described in Sec. II B. The Zarges box is equipped with one camera and one LED light panel for each DU, and the camera image for a certain DU is displayed on the corresponding laptop. Any loss in functionality in any of these, camera, light, or ventilation, is the reason for a shutdown of the DU concerned for the rest of the flight day or until the function has been safely restored.

The main scientific function is the dipping motion. The laptops are each connected to a dipping motion controller (Newport SMC100CC), which is connected to the linear dipping drive (Newport UTS100CC), inside the Zarges box. All parameters for the dipping motion are set in the software (Newport SMC100), which communicates with the controllers. These parameters include the dipping/withdrawal speed (0 mm/s–40 mm/s), the dipping distance (0 mm–100 mm), and the initiation of the coating sequence that consists of dipping, hold time in the dipped position, and withdrawal.

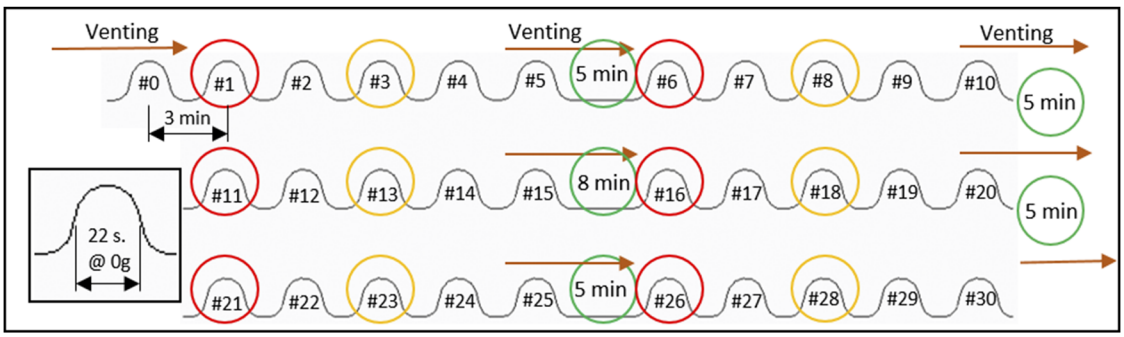

FIG. 7. A schematic description of the performed parabolas and ventilation for the dipping units. Red circles indicate dipping of the first unit and yellow circles the second unit. Green circles indicate fork change in both DUs. Arrows indicate the minimum time for venting of the DUs. The time between the start of two adjacent parabolas is 3 min, and 22 s of microgravity is achieved in each parabola. Adapted with permission from Novespace User Guide, UG-2017-01, 2017. Copyright 2017 Novespace.[30]

The hold time is always 0.5 s, but the withdrawal speed is changed between each set of coatings, being a crucial parameter for the film formation. In these experiments, the used withdrawal speeds were 5 mm/s, 10 mm/s, 17 mm/s, 20 mm/s, and 40 mm/s.

As described in Sec. II A, a slider seals the vials in the DUs. Servomotors with indicator flags visible in the camera images make it possible to monitor the movement of the sliders. Initiation of moving the sliders is done manually on a control panel mounted on the control rack, and for safety, the power to the servomotors is turned off when the sliders are in the closed position.

D. Experiment preparation

Solutions that are to be used in flights are prepared the day before and stirred overnight. In the morning of the flight day, ~8 ml of solution is filled in each vial with the vials mounted in the DU, and the sealing slider above the vials is closed. Clean glass substrates are mounted on the dipping forks. These steps are performed in a ground laboratory with all handling of volatile solvents done in a ventilated fume hood. After the DUs have been sealed and leak-tested, the forks and DUs are transported to the aircraft in custom-designed suitcases. The two DUs are mounted in the Zarges box, 10 forks are hanged on one of the fork racks in the Zarges box, and two are mounted in the DUs. Upon mounting the DUs in the Zarges box, the DUs are also aligned, connected to ventilation, and grounded. After the flight, all forks and the DUs are put back in their suitcases and transported back to the ground laboratory for dismounting and cleaning of the DUs.

E. Experimental execution

A typical experiment is performed as follows. The ventilation for the Zarges box and the DUs is open during lift-off. The ventilation for the Zarges box is always kept fully open, while the ventilation for the DUs is closed during dipping and completion of the parabola. The reason for closing the ventilation to the DUs during dipping is to avoid disturbance on the drying films due to air streams.

After reaching the cruise level, the integrity of the Zarges box and DUs is checked through a window in the Zarges box before the electronics is turned on. The laptops are started together with the cameras and internal illumination, and the integrity of the DUs is again checked. After setting up communication between the laptops and the linear drives, a short test is performed to check the communication.

In detail, a coating is performed by first opening the sealing slider and checking that the slider is in an open position via cameras, second, initiating the coating sequence that will dip and withdraw the five substrates in one DU in one controlled motion, and third, closing the sealing slider and check that it has reached the closed position. Since the drying of the films shall occur in microgravity, the coating sequence is initiated during the pull-up phase, before the microgravity phase. Different speeds were used, and the coating sequences were thus initiated 15 s–40 s before injection to microgravity. These times were chosen to allow the sealing slider to close, as close as possible to the microgravity phase. For example, at 40 mm/s dipping speed, the motion takes 15 s. Opening plus closing of the slider takes 6 s, and the time from pull-up to injection is 20 s. Thus, the sequence is started 5 s before the pull-up starts to allow a few seconds margin before reaching the microgravity phase of the parabola.

In Fig. 7, the timeline for all six sets of parabolas is shown. After using DU 1 (red circle) and DU 2 (yellow circle), the forks in both DUs are replaced with the unused forks in the short break between sets (green circle). During this change, the cover of the Zarges box is opened, meaning that the second containment for solvent vapors is broken temporarily. Before opening, the integrity of the vials is checked via the camera, and all vent lines must have been fully open for at least one parabola. It is worth noting that some of the solvents used would have caused an unpleasant smell in the airplane cabin if released in the Zarges box while it was opened. During flight, no smell was detected outside of the Zarges box at any time, thus concluding that the experimental equipment performed well regarding solution containment and ventilation.

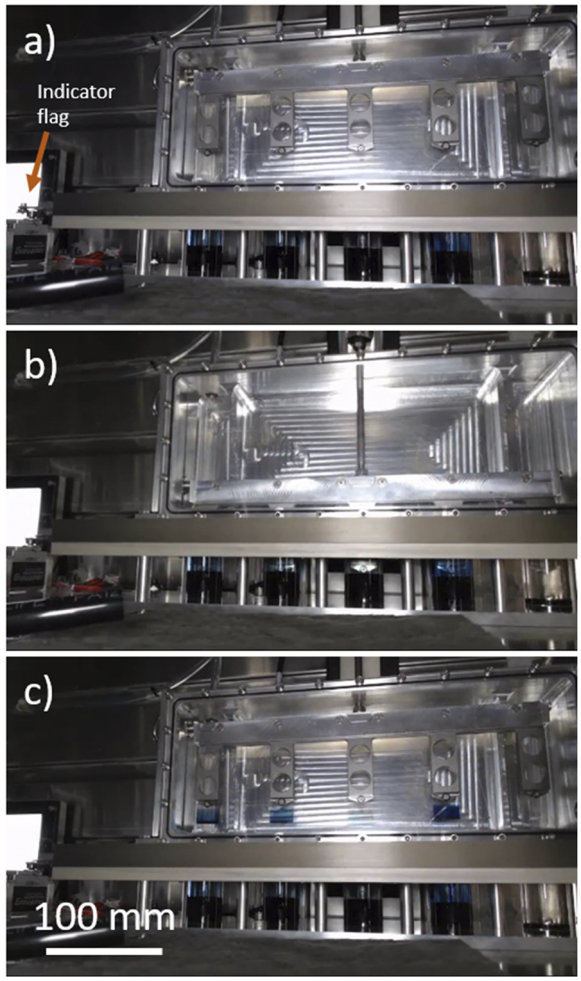

FIG. 8. Snapshots from the surveillance camera inside the Zarges box, showing one dipping unit in operation during the parabola flights. (a) Starting position with the sealing slider in the closed position, as indicated by the flag to the far-left. (b) The substrates dipped in the solutions. (c) The withdrawn substrates with clearly visible blue films. Multimedia view: https://doi.org/10.1063/5.0018223.1

The standard procedure we employed is to use the first and third parabola in each set of parabolas to perform coating in one DU during each, leaving the second parabola for preparation if needed. Occasionally, the first and second parabolas or the second and third parabolas were used, still leaving sufficient ventilation time for the DUs before change of forks (see Sec. II A). As illustrated in Fig. 7, using the last parabola of each set for ventilation of the Zarges box and the DUs is a minimum requirement.

F. Experimental performance

During the 70th ESA Parabolic Flight Campaign, all equipment performed well, apart from some software issues. Due to bad weather conditions, one parabola was interrupted before injection, resulting in microgravity conditions while one of the sealing sliders was still open. The interrupted parabola resulted in solution flowing into the upper part of one DU, and consequently, this DU was closed down for the rest of the flight day with the ventilation open. The gravity fluctuations, continuously measured in the aircraft, during this parabola set (11a-15) are shown in Fig. SU1 of the supplementary material. The interrupted parabola, 11a, was replaced by a new, 11b, and thus, the set was completed.

Thin films were prepared during flight using solutions in four different solvents: chlorobenzene, *o*-dichlorobenzene, fluorobenzene, and *o*-difluorobenzene. The second variable was the blend ratio between the two solutes, TQ1 and $PC_{70}BM$, and the third one was the solute concentration. In addition, as a fourth variable, the withdrawal speed was varied. During this flight campaign, 130 dip-coated samples were produced and brought to in-house laboratories for characterization with several methods.

In Fig. 8 (Multimedia view), the snapshots from one of the cameras inside the Zarges box are shown. The operation of the DU in one set of coatings is shown, from top to bottom: The fork is in the starting position before dipping, glass substrates fully dipped, and coated substrates withdrawn from the vials. In the last snapshot [panel (c)], the substrates still have a wet thin film of solution, clearly visible by its color.

G. Results

The obtained dry coatings were primarily evaluated by microscopy methods. Peak Force Tapping Mode AFM was performed using a Bruker Multimode 8 with a Si/SiN tip to characterize the thin films formed under microgravity conditions and to compare them with the films prepared on ground.

The AFM characterization was used to study the surface morphology of the films by imaging different parts of the film with respect to the withdrawal direction. In Fig. 9, such a series is shown, showing the surface morphology of dip-coated TQ1:$PC_{70}BM$ films prepared from a 10 mg/ml solution in chlorobenzene and with the donor:acceptor ratio set to 1:3 weight-by-weight. The withdrawal speed was 17 mm/s for all images, and the average domain region sizes are given in each image. We note indications of a slower phase separation process in the films prepared under microgravity

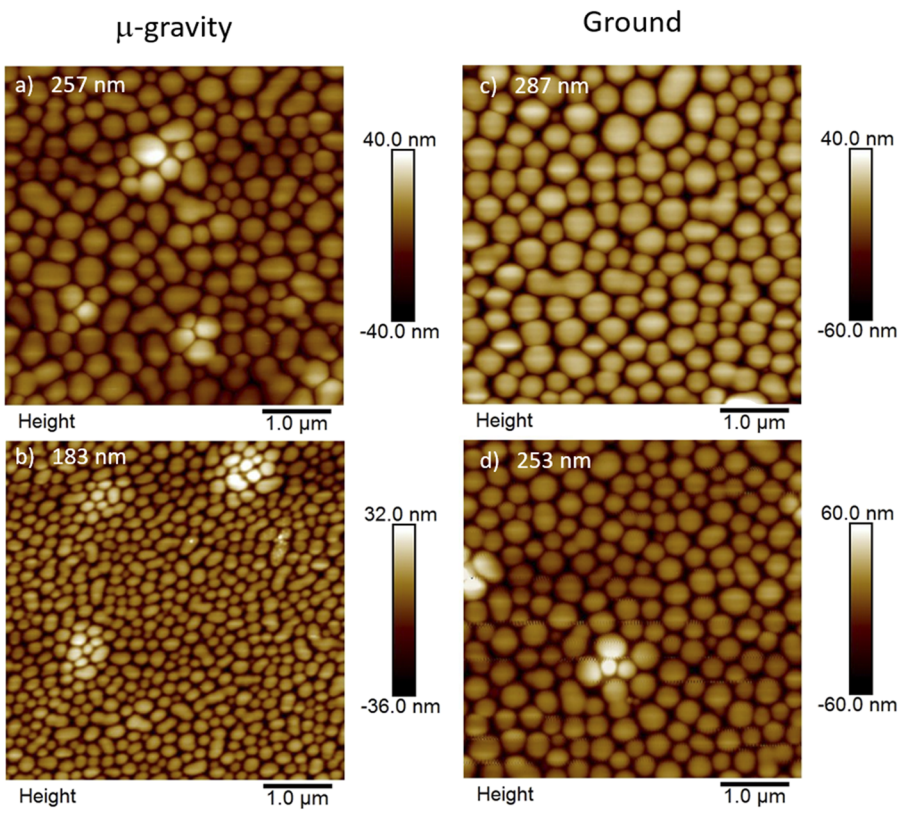

FIG. 9. Peak Force Tapping Mode AFM height images showing the surface morphology of dip-coated blend films. (a) and (b) show a sample coated under microgravity, while (c) and (d) show a sample coated on ground. (a)/(c) and (b)/(d) are taken at similar positions with respect to the depth of dipping. The films are made from a 10 mg/ml solution of TQ1:$PC_{70}BM$ (ratio 1:3 w/w) in chlorobenzene, and the withdrawal speed was 17 mm/s. The average domain region size is given in each image.

conditions as compared to the films prepared on ground because the films prepared under microgravity conditions exhibit smaller domain regions at comparable film positions. These results show that phase-separated films can be produced from solution under microgravity conditions with our custom-built equipment, that the films are of comparable quality as those prepared at ground, and that a difference in the films appear as a result of the lower gravity during film drying. Further investigations and analysis of the produced films are to be reported in a separate publication.

III. CONCLUSIONS

Using a custom-built experimental setup, we have shown that it is possible to produce dip-coated thin films of polymer blends from solution under microgravity conditions. The equipment built for dip coating in volatile solutions onboard an airplane worked excellently and safely. Safety was tested during flight in a real case due to unexpected gravity fluctuations. The equipment was able to prevent any solvent or solvent gases to leak from the first containment, even though the solvent flowed out of the vials into the dipping unit. Inspection by AFM shows that the dry films are of similar quality as those prepared on ground, but with a difference in the domain size. This difference can be related to a slowed down phase separation under microgravity conditions.

It should be mentioned that there is no direct inspection of the drying process in the present configuration of the experimental setup. This leads to a possible uncertainty concerning if the deposited liquid film is completely dried under the microgravity phase of one parabola or not. We cannot completely rule out the influence of the increased gravity during the pull-up or pull-out phases, with hypergravity conditions, on the final dry film morphology. In an upcoming parabolic flight campaign, the experimental setup will be modified to allow *in situ* monitoring of the drying process through a schlieren setup. We also plan for participation in sounding rocket experiments, with a microgravity phase of several minutes. Such experiments would allow complete drying under microgravity conditions with full certainty and will also serve as a control of the results obtained under parabolic flight microgravity conditions.

SUPPLEMENTARY MATERIAL

See the supplementary material for the graph showing the gravity fluctuations during a parabola set, including the interrupted pull-up sequence (Fig. SU1).

ACKNOWLEDGMENTS

The experiments were performed during the 70th ESA Parabolic Flight Campaign. The authors are grateful to the Novespace staff, especially Brian Verthier and Frédéric Gai, who contributed with invaluable input all through the design process as well as during the flight campaign. The authors sincerely thank Dr. Dargie Deribew for valuable discussions, Dr. Guillaume Wantz, University of Bordeaux, France, for discussions and taking care of practical issues during the flight campaign, and Sandra Hultmark, Chalmers University of Technology, Gothenburg, Sweden, for testing the equipment and taking part in the flight campaign. The workshop staff at Karlstad University is gratefully acknowledged for help in the assembly process and Mikael Andersén for vital assistance throughout the whole project.

This work was funded by the Swedish National Space Agency (Grant Nos. 185/17 and 174/19) and the Knut och Alice Wallenbergs Stiftelse (Grant No. 2016.0059).

DATA AVAILABILITY

The data that support the findings of this study are available from the corresponding author upon reasonable request.

REFERENCES

[1] C. Lindqvist, E. Moons, and J. van Stam, Materials **11**(11), 2068 (2018).
[2] N. Uranbileg, C. Gao, C. Yang, X. Bao, L. Han, and R. Yang, J. Mater. Chem. C **7**(35), 10881–10890 (2019).
[3] C. J. Brabec, S. Gowrisanker, J. J. M. Halls, D. Laird, S. Jia, and S. P. Williams, Adv. Mater. **22**(34), 3839–3856 (2010).
[4] C. Zheng, I. Jalan, P. Cost, K. Oliver, A. Gupta, S. Misture, J. A. Cody, and C. J. Collison, J. Phys. Chem. C **121**(14), 7750–7760 (2017).
[5] C. Zheng, D. Bleier, I. Jalan, S. Pristash, A. R. Penmetcha, N. J. Hestand, F. C. Spano, M. S. Pierce, J. A. Cody, and C. J. Collison, Sol. Energy Mater. Sol. Cells **157**, 366–376 (2016).
[6] S. B. Darling and F. You, RSC Adv. **3**(39), 17633–17648 (2013).
[7] R. Søndergaard, M. Hösel, D. Angmo, T. T. Larsen-Olsen, and F. C. Krebs, Mater. Today **15**(1), 36–49 (2012).
[8] G. Yu, J. Gao, J. C. Hummelen, F. Wudl, and A. J. Heeger, Science **270**(5243), 1789 (1995).
[9] J. Nelson, Mater. Today **14**(10), 462–470 (2011).
[10] C. McDowell, M. Abdelsamie, M. F. Toney, and G. C. Bazan, Adv. Mater. **30**(33), 1707114 (2018).
[11] H. Lee, C. Park, D. H. Sin, J. H. Park, and K. Cho, Adv. Mater. **30**(34), 1800453 (2018).
[12] S. Mukherjee, C. M. Proctor, J. R. Tumbleston, G. C. Bazan, T.-Q. Nguyen, and H. Ade, Adv. Mater. **27**(6), 1105–1111 (2015).
[13] S. Nilsson, A. Bernasik, A. Budkowski, and E. Moons, Macromolecules **40**(23), 8291–8301 (2007).
[14] R. Hansson, L. K. E. Ericsson, N. P. Holmes, J. Rysz, A. Opitz, M. Campoy-Quiles, E. Wang, M. G. Barr, A. L. D. Kilcoyne, X. Zhou, P. Dastoor, and E. Moons, J. Mater. Chem. A **3**(13), 6970–6979 (2015).
[15] R. S. Gurney, D. G. Lidzey, and T. Wang, Rep. Prog. Phys. **82**(3), 036601 (2019).
[16] F. Zhao, C. Wang, and X. Zhan, Adv. Energy Mater. **8**(28), 1703147 (2018).
[17] L. Ye, H. Hu, M. Ghasemi, T. Wang, B. A. Collins, J.-H. Kim, K. Jiang, J. H. Carpenter, H. Li, Z. Li, T. McAfee, J. Zhao, X. Chen, J. L. Y. Lai, T. Ma, J.-L. Bredas, H. Yan, and H. Ade, Nat. Mater. **17**(3), 253–260 (2018).
[18] N. P. Holmes, H. Munday, M. G. Barr, L. Thomsen, M. A. Marcus, A. L. D. Kilcoyne, A. Fahy, J. van Stam, P. C. Dastoor, and E. Moons, Green Chem. **21**(18), 5090–5103 (2019).
[19] A. D. Narendranath, J. C. Hermanson, R. W. Kolkka, A. A. Struthers, and J. S. Allen, Microgravity Sci. Technol. **26**(3), 189–199 (2014).
[20] S. Bamberger, D. E. Brooks, J. M. Van Alstine, J. M. Harris, and R. S. Snyder, in *Separations Using Aqueous Phase Systems*, edited by D. Fisher and I. A. Sutherland (Springer, Boston, MA, 1989), pp. 281–286.
[21] A. E. Bailey, W. C. K. Poon, R. J. Christianson, A. B. Schofield, U. Gasser, V. Prasad, S. Manley, P. N. Segre, L. Cipelletti, W. V. Meyer, M. P. Doherty, S. Sankaran, A. L. Jankovsky, W. L. Shiley, J. P. Bowen, J. C. Eggers, C. Kurta, T. Lorik, P. N. Pusey, and D. A. Weitz, Phys. Rev. Lett. **99**(20), 205701 (2007).
[22] M. Paley and D. Frazier, Proc. SPIE **2809**, 114–124 (1996).
[23] J. Whitehead and M. Chandler, Proc. SPIE **3123**, 128–134 (1997).

[24]J. van Stam, R. Hansson, C. Lindqvist, L. Ericsson, and E. Moons, Colloids Surf., A **483**, 292–296 (2015).
[25]J. van Stam, C. Lindqvist, R. Hansson, L. Ericsson, and E. Moons, Proc. SPIE **9549**, 95490L (2015).
[26]V. Blazinic, L. K. E. Ericsson, I. Levine, R. Hansson, A. Opitz, and E. Moons, Phys. Chem. Chem. Phys. **21**(40), 22259–22271 (2019).
[27]E. Wang, L. Hou, Z. Wang, S. Hellström, F. Zhang, O. Inganäs, and M. R. Andersson, Adv. Mater. **22**(46), 5240–5244 (2010).
[28]I. Cardinaletti, T. Vangerven, S. Nagels, R. Cornelissen, D. Schreurs, J. Hruby, J. Vodnik, D. Devisscher, J. Kesters, J. D'Haen, A. Franquet, V. Spampinato, T. Conard, W. Maes, W. Deferme, and J. V. Manca, Sol. Energy Mater. Sol. Cells **182**, 121–127 (2018).
[29]L. K. Reb, M. Böhmer, B. Predeschly, S. Grott, C. L. Weindl, G. I. Ivandekic, R. Guo, C. Dreißigacker, R. Gernhäuser, A. Meyer, and P. Müller-Buschbaum, Joule **4**(9), 1880–1892 (2020).
[30]Novespace User Guide UG-2017-01, 2017.